MATHEMATICAL MODELLING OF THERMAL EVOLUTION AS A TOOL FOR ENHANCING STEEL ROUGH ROLLING*

Antonio Adel dos Santos[1]
Bruno Alves Resende[2]

Abstract

Temperature, microstructure and dimensions are the main material parameters to be controlled during hot rolling of steel. Although thermal mathematical models have long been developed and applied for hot strip rolling, each Hot Strip Mill (HSM) must have its own model adapted to its facilities. Thus, a mathematical model for temperature evolution during rough rolling has been developed for the Usiminas HSM at Ipatinga Plant. The model achieved a high level of accuracy, which was assessed by comparing measured values of temperature at the hot strip mill entry with the calculated ones, the difference ranging from 9°C to 17°C. Application examples have shown that the slab can be occasionally stopped before start of rolling for as long as a couple of minutes without compromising its further processing. On the other hand, if the transfer bar stops after rough rolling even for short time, further processing in the HSM can be hindered, due to excessive temperature drop. In case of such abnormal line stop, the model can be used as a tool for decision-making to either continuing the planned rolling schedule or to changing the route, thus improving the overall rolling process.

Keywords: Mathematical modelling; thermal evolution; rough rolling.

[1] *Metallurgical Engineer, DSc., R&D Center, Usiminas, Ipatinga, MG, Brazil.*
[2] *Mechanical Engineer, MSc., R&D Center, Usiminas, Ipatinga, MG, Brazil.*

** Technical contribution to the 11th International Rolling Conference, part of the ABM Week 2019, October 1st-3rd, 2019, São Paulo, SP, Brazil.*

1 INTRODUCTION

The knowledge and control of material temperature during hot rolling process is crucial for productivity, product quality and production costs. Mathematical models together with online temperature measurements are devised to achieve, simultaneously, these requisites within their tolerance limits. The mathematical models are based on fundamental laws of heat transfer between the material and the ambient, taking into account the characteristics of the processing line and the processed materials.

The pioneering work by Hollander [1] on thermal evolution in the hot strip rolling has laid the basis for further progress in this field. Nowadays, ample technical literature about heat transfer on hot rolling process are available, see, for example, regarding the reheating process [2,3], hot deformation [4], and strip cooling in the run-out table [5,6]. Despite the wealth of information, details of model applications to industrial process can be hardly found in literature. At least in part, this can be attributed to the fact that, in each steel plant, the mathematical models are proprietary information that are prevented from publishing.

Moreover, the models need to be designed to meet the specific characteristics of each mill facilities and material processed in each steel plant, so that they can provide reliable and useful results.

Thus, the present paper presents the basic features of the thermal mathematical model developed to simulating the rough rolling phase in the hot strip mill (HSM) of Usiminas in Ipatinga. So far, the model can provide useful information for decision making about continuing the rolling process or to changing the schedule in case the slab/piece has to wait on the roller table due to abnormal line stop. In future, the temperature model will be coupled with a deformation model and a microstructure model, in order to give overall information about the material status during rough rolling.

2 MATHEMATICAL MODEL

2.1 Heat transfer equations

The model considers one-dimensional heat transfer conduction through the piece thickness, as given by Fourier equation (1). Material properties density, ρ, specific heat, C, and thermal conductivity, k, are temperature dependent, which, in turn, is time, t, and position, x, dependent. To complete nomenclature, S is the heat source or heat sink by volume unit.

$$[T(t,x)]C[T(t,x)]\frac{\partial T(t,x)}{\partial t} = \frac{\partial}{\partial x}\left\{k[T(x,t)]\frac{\partial T(t,x)}{\partial x}\right\} + S \qquad (1)$$

In order to take thermal conductivity out of the temperature derivative, Eyres transformation is applied as given by equation (2), where k_d is the standard conductivity and ϕ is the converted temperature. k_d is usually taken as the conductivity at 0°C.

$$\phi = \int_{\phi_d}^{\phi} \frac{k}{k_d} dT \qquad (2)$$

Another useful transformation is related to specific heat and enthalpy, H, according to equation (3).

$$C = \frac{\partial H}{\partial \phi} = \frac{\partial H}{\partial t} \cdot \frac{\partial t}{\partial \phi} \qquad (3)$$

Applying definitions (2) and (3) into equation (1), removing the parenthesis (t,x) for sake of simplicity, and after some algebrism a lean differential equation as given by (4) is attained.

$$C\frac{\partial H}{\partial t} = \frac{k_d}{\rho}\frac{\partial^2 \phi}{\partial x^2} + \frac{S}{\rho} \qquad (4)$$

The partial differential equation (4) is solved by the finite difference method, explicit formulation as set by equation (5), where Δt denotes the time interval between successive calculations and Δx means the node spacing in the numerical solution mesh. Subscript i stands for node number.

$$H_{t+\Delta t} = H_t + \frac{2k_d \Delta t}{\rho \Delta x_i}\left[\frac{\phi_{i+1}}{\Delta x_{i+1} + \Delta x_i} + \frac{\phi_{i-1}}{\Delta x_i + \Delta x_{i-1}} - \phi_i\left(\frac{1}{\Delta x_{i+1} + \Delta x_i} + \frac{1}{\Delta x_i + \Delta x_{i-1}}\right)\right] \quad (5)$$

Equation (5) is applied to internal nodes. For surface nodes, a heat balance is done in order to get the final difference equation, as given by (6).

$$H_{t+\Delta t} = H_t + \frac{2.k_d \Delta t(\phi_{i+1} - \phi_i)}{\rho \Delta x_i} - \frac{q_s \Delta t}{\rho \Delta x_i} + \frac{S_i \Delta t}{\rho} \quad (6)$$

Given that an explicit solution scheme was chosen, a criterion to limit the solution time interval must be used in order to guarantee its convergence. Equations (7) and (8) are the convergence criteria applied to internal and surface nodes, respectively. α_d is the standard thermal diffusity.

$$\Delta t \le \frac{1}{\frac{2\alpha_d}{\Delta x_i}\left(\frac{1}{\Delta x_{i+1} + \Delta x_i} + \frac{1}{\Delta x_i + \Delta x_{i-1}}\right)} \quad (7)$$

$$\Delta t \le \frac{1}{2\alpha_d\left[\frac{h_s}{2k_d \Delta x_1} + \frac{1}{\Delta x_1(\Delta x_1 + \Delta x_2)}\right]} \quad (8)$$

Finally, boundary conditions are needed for solving the discretization equations, in terms of heat flux and heat transfer coefficient from piece surface to the ambient, q_s and h_s, in equations (6) and (8), respectively. The heat flux by radiation was given by the Stefan-Boltzmann law, equation (9), where T_s and T_a are surface and ambient temperature, respectively, in K; σ is the Stefan-Boltzmann constant; ε, the steel emissivity; F_{rad} is introduced as a fitting factor.

$$qs_{rad} = \sigma\varepsilon[T_s(t)^4 - T_a^4]F_{Rad} \quad (9)$$

For natural convection the simple expression given by Holman [7] was used, equation (10). Here, the multiplying factor, a, is set to 2.8 and 1.4 for top and bottom surface, respectively. F_{Nat} is a factor introduced to fitting the model.

$$h_{s\_nat} = a[T_s(t) - T_a]^{0.25}F_{Nat} \quad (10)$$

For forced convection applied to cooling under the descaling sprays the heat transfer coefficient ($W.m^{-2}.K^{-1}$) was given by equation (11), where *w* stands for water density ($L.m^{-2}.min^{-1}$) and F_{For} is the fitting factor.

$$h_{s-for} = 124.6w^{0.793}.10^{-0.00154.T_s(t)} \quad (11)$$

During the rolling pass, under the arc of contact, three additional heat parcels were accounted for in the thermal model: heat generation due to both deformation and the friction with work rolls, allocated in the source term S; heat transfer to work roll surface, allocated in the heat transfer coefficient.

2.2 Time-position scheme

Figure 1 shows the layout of Usiminas HSM in Ipatinga, where the dashed line rectangle highlights the roughing area corresponding to the thermal model domain. Initial thermal condition of the slab is assumed as a parabolic temperature distribution across its thickness, based on discharging temperature calculated by the furnace model. After discharging, the slab passes through the primary scale breaker, HSB, going to the rolling phase. Because the two roughing mills are reversible an abstraction was done concerning the sequence of deformation pass. As shown in Figure 2, the model considers virtual and repetitive positions for the roughers along the rolling schedule. Each rougher, R1 and R2, may apply any number of pass in the model. From the furnace exit until the FM entry pyrometer position, TS, the domain is divided into 14 zones, each one having a varied number of sectors. Each sector is characterized by a specific heat transfer mode.

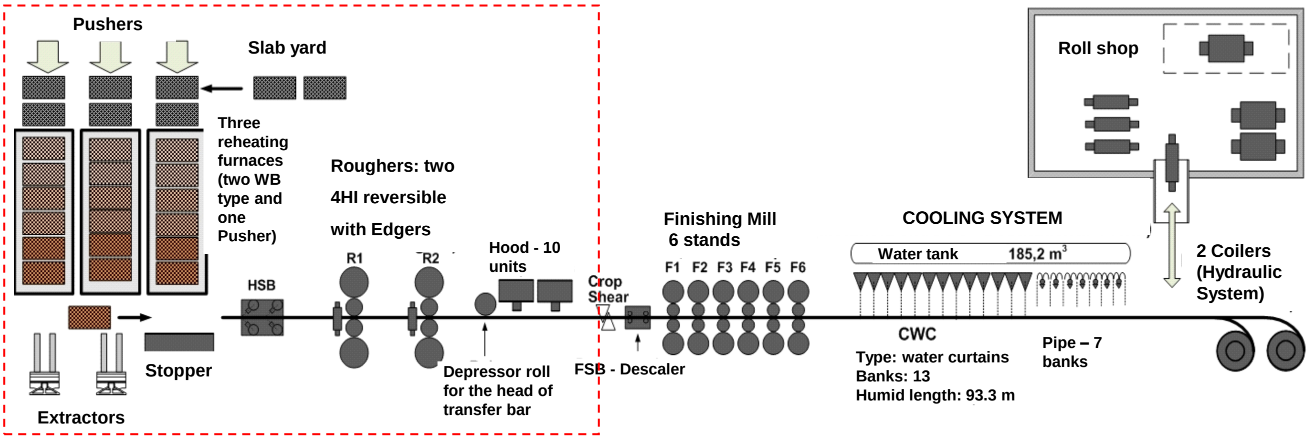

Figure 1. Layout of USIMINAS HSM at Ipatinga Plant highlighting the model domain area.

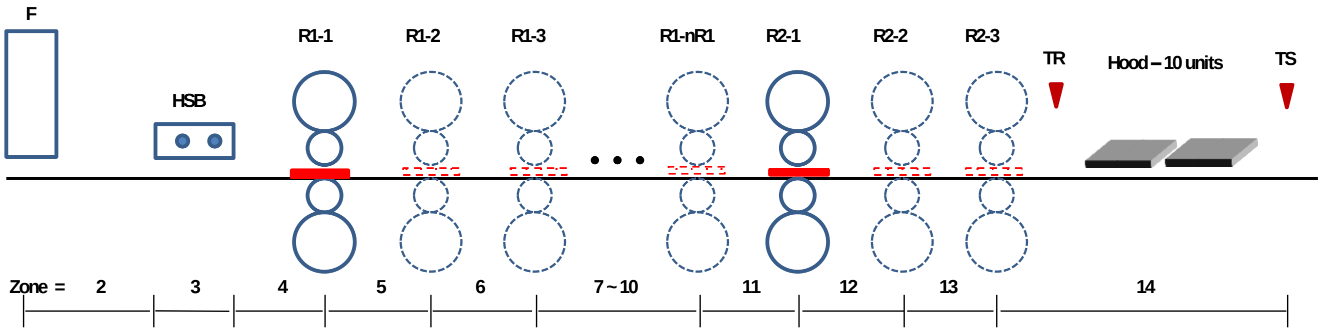

Figure 2. Virtual location of the roughers during the pass sequence of rough rolling conceived for model's purpose. Zone 1 is the discharging position.

The model calculates the thermal evolution in head, middle and tail of the piece. Hence, a tracking scheme is associated to each position during rolling, considering that the rolls bite either the head or the tail of the piece, depending on the pass direction.

2.3 Input data

To run the model the following groups of input data were needed: (1) slab dimensions and chemical composition; (2) slab discharging temperature and residence time in the furnace; (3) number of reduction passes; (4) data for each pass, like gage, pass time, interpass time, rolling load, speed, descaling on or off.

Besides those variables cited in items from (1) to (4), to run the model requires an additional set of fixed parameters related to line configuration in terms of lengths and distance of events, like discharging, HSB descaling, pass descaling, hood length, pyrometers, etc..

3 MODEL RESULTS

3.1 Model output

The model outputs a table containing temperature and scale thickness calculated along the rolling time. Values of temperature are gotten on the surface, TS, center, TC, and the average across the thickness, TM. Regarding the scale growth model, the details are given in a paper presented previously [8] and will not be shown here.

Table 1 gives a summary of values of piece temperature and scale thickness at specific locations along the rolling schedule, for the head, middle and tail of the piece, as an example.

Table 1. Calculated values of temperature and scale thickness at specific locations along the roughing process. Example for a slab rolled with 7 passes in R1 and 3 in R2, the second pass in R2 being dummy

Position	Coil: 840918597							Location								
	Variable	Disch.	HSB entry	HSB exit	R1-1	R1-2	R1-3	R1-4	R1-5	R1-6	R1-7	R2-1	R2-2	R2-3	TR	TS
Head	TM (°C)	1224	1207	1206	1203	1198	1195	1189	1187	1177	1164	1123		1043	1045	1010
	TS (°C)	1236	1111	1098	1077	1063	1049	1052	1054	1057	1059	1037		1002	1010	984
	TC (°C)	1218	1219	1219	1219	1221	1224	1227	1230	1228	1217	1166		1064	1065	1022
	Scale thickness (μm)				9.9	48.5	8.0	44.0	47.4	61.0	67.8	10.0		70.6		67.6
Middle	TM (°C)	1224	1205	1205	1201	1198	1193	1189	1184	1178	1160	1114		1036	1038	996
	TS (°C)	1237	1107	1094	1073	1063	1047	1051	1054	1056	1057	1030		995	1004	971
	TC (°C)	1217	1218	1218	1218	1221	1223	1227	1229	1229	1212	1156		1057	1058	1008
	Scale thickness (μm)				9.7	42.7	7.9	37.1	49.8	56.9	71.0	9.6		67.6		66.5
Tail	TM (°C)	1224	1204	1204	1200	1198	1191	1190	1182	1179	1155	1105		1029	1032	983
	TS (°C)	1237	1103	1090	1070	1062	1045	1048	1053	1054	1054	1023		989	998	958
	TC (°C)	1217	1218	1218	1218	1221	1223	1227	1228	1230	1208	1146		1050	1051	994
	Scale thickness (μm)				9.5	36.2	7.8	29.1	52.0	52.6	73.9	9.1		64.9		65.3

Figure 3 shows a graph with the evolution of temperature and scale thickness, as an example, for the piece whose results were given in Table 1. Typical abrupt drop of surface temperature occurring under the descaling jets as well as in the roll bite can be noted. Once the penetration depth of temperature drop into material layers is very low, internal temperatures hardly change due these events, and a quick growth back is observed. On the contrary, during the deformation pass a jump was observed in internal temperature values due to heat released by deformation.

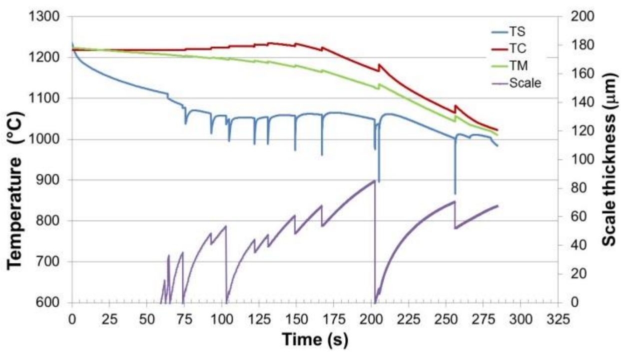

Figure 3. Evolution of calculated temperature and secondary scale thickness during rough rolling.

3.2 Model validation

For validation, calculated temperatures were compared to measured values in 12 rolled transfer bars at positions TR and TS, Figure 2. The fitting factors in equations (9), (10) and (11) were used for model tuning.

Firstly, a comparison was made of calculated and measured processing times from furnace discharging until the pyrometer TS, at finish mill entry. The measured time was obtained from DAS (data acquisition system) records. It can be noted in Figure 4 that the calculated time by the model matches well the measured one, except for the first transfer bar. No reason was found for such a big difference, so the calculated value was accepted as the reliable one.

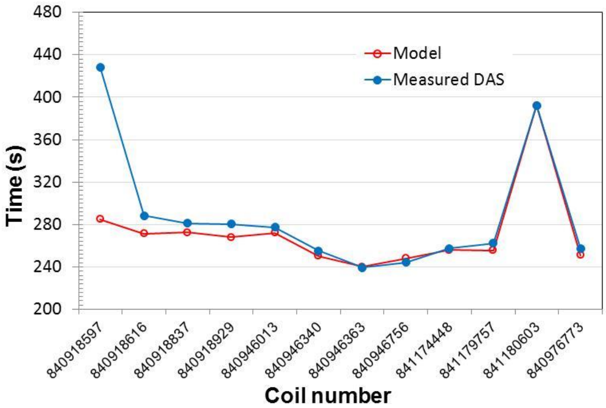

Figure 4. Comparison between calculated and measured processing time.

Secondly, temperature validation was realized. The graphs in Figure 5 show comparisons of calculated and measured surface temperature at location TR (R2 exit) in middle of the piece, and for head, middle and tail of the transfer bar at TS pyrometer. Considering the usual temperature tolerances in hot rolling process, for prediction and control purposes, the model accuracy is satisfactory. In general, values calculated by the model tend to be more stable than the measured ones among the rolled pieces.

Estimates of model accuracy are given in table 2 in terms of one standard deviation for the calculated temperatures in respect to measured ones. As seen in the table and in the graphs, the bigger error lies at R2 exit. All error estimates were in the range 9°C to 17ºC, which is very acceptable.

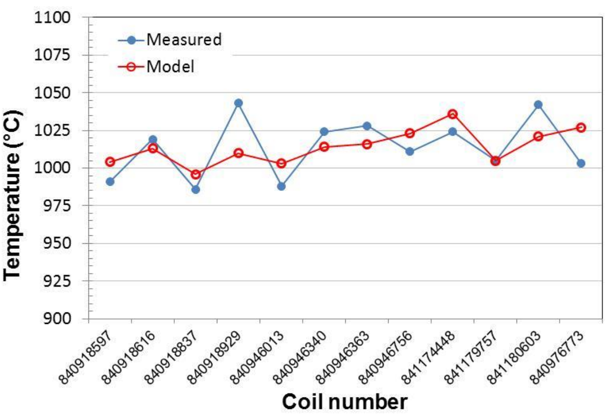

(a) TR middle

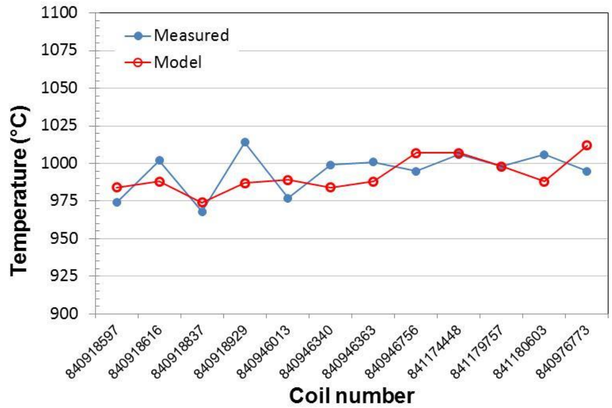

(b) TS head

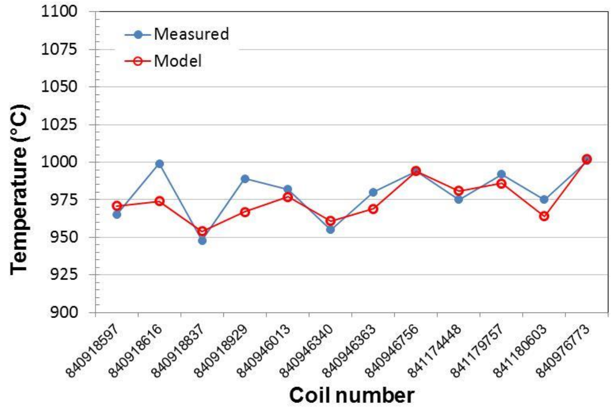

(c) TS middle

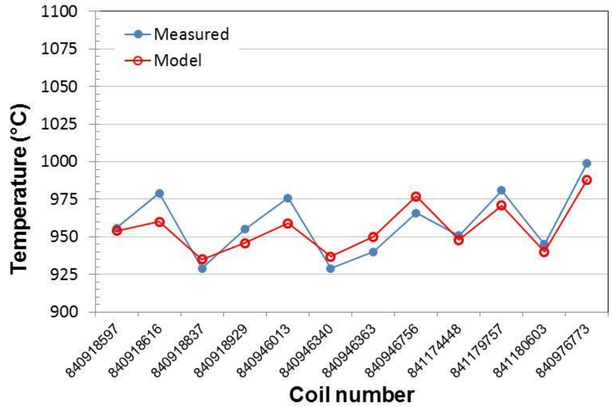

(d) TS tail

Figure 5. Calculated and measured temperature values in 12 transfer bars at location R2 exit and HSM entry, for head, middle and tail of transfer bar.

Table 2. Estimates of model errors

Error measure	TR - middle	TS - head	TS - middle	TS - tail
Standard deviation (°C)	17.0	14.4	10.9	10.3
Average error (°C)	14.0	12.1	8.8	9.3

Due to the lack of online measurements, the validation of secondary scale thickness was missing. It is worth noting that the calculated thickness lies within the known range for secondary scale, from 40 µm to 80 µm. So far in the model, this calculation may be used as a tendency only.

4 MODEL APPLICATION EXAMPLES

At present, the model can be run offline. In future, it will be implemented online so that actions that are nowadays taken by operators manually would be automatized and based on the simulated results. Here, a couple of examples are given to illustrate the model capability to help the decision-making by the operator.

4.1 Abnormal slab stop

The slab corresponding to the coil number 841180603 stopped for 148 s at HSB entry (Figures 1 and 2) before starting to be rolled in R1. Without the stoppage the processing time would be 244.2 s in the head. So the model was run using both 244.2 s and 392.2 s for both conditions, without and with slab stop.

The effect of stop on piece temperatures along the rolling process can be seen in Table 3. For the first 5 passes in R1 the average temperature across the transfer bar thickness considering slab stop is about 30°C lower than that without stop. This is a negligible difference for rolling loads purpose, because the mean flow stress at so high temperatures does not change much. The relatively low temperature drop is due to high material thickness and to the coarse scale layer covering the slab surface, which decreases heat loss. From start of rolling in R1 on, the temperature difference between conditions without and with stoppage is still lower, reaching about 15°C, which does not compromise further processing in HSM.

Table 3. Example of calculated temperatures at the piece head along the rough rolling, without and with slab stop before HSB

Condition	Coil: 841180603							Location								
	Variable	Disch.	HSB entry	HSB exit	R1-1	R1-2	R1-3	R1-4	R1-5	R1-6	R1-7	R2-1	R2-2	R2-3	TR	TS
Without stop	TM (°C)	1225	1207	1206	1202	1197	1195	1187	1184			1149		1065	1073	1027
	TS (°C)	1246	1115	1102	1080	1054	1064	1068	1071			1062		1022	1042	1003
	TC (°C)	1214	1216	1216	1216	1219	1225	1229	1231			1193		1086	1090	1039
	Scale thickness (µm)				10.5	3.2	37.8	58.5	5.6			9.5		80.4		70.6
With stop	TM (°C)	1225	1174	1174	1170	1166	1165	1159	1157			1125		1046	1055	1012
	TS (°C)	1246	1043	1030	1015	997	1014	1028	1036			1039		1005	1025	988
	TC (°C)	1214	1214	1214	1213	1215	1218	1217	1216			1170		1067	1071	1023
	Scale thickness (µm)				7.0	2.2	27.5	44.4	4.5			8.2		71.8		63.5

4.2 Transfer bar stoppage

The second model application example considers the stop of the transfer bar before entering the finishing mill. For a given transfer bar, the transportation time from R2 to TS location is 34 s for the head. However, this transfer bar had to wait for additional 48 s before travelling to the HSM.

Table 4 shows a comparison between the predicted temperatures in the transfer bar tail, without and with the stop. It is seen that less than 1 min stop causes a meaningful temperature drop of 57°C in the tail, rendering further processing in HSM under the planned schedule unfeasible, because the temperature was too low. Off course, the big temperature difference is due to the low material thickness at the final stage of rough rolling that leads to high heat loss to ambient.

The model will be implemented online as the next step, so the material temperature will be calculated at relevant time events, giving aid for decision-making about the course of rolling schedule.

Table 4. Example of calculated temperatures at the head of rolling piece along the line, without and with transfer bar stop after the R2

Condition	Coil: 840918597	Location														
	Variable	Disch.	HSB entry	HSB exit	R1-1	R1-2	R1-3	R1-4	R1-5	R1-6	R1-7	R2-1	R2-2	R2-3	TR	TS
Without stop	TM (°C)	1224	1204	1204	1200	1198	1191	1190	1182	1179	1155	1105		1029	1032	979
	TS (°C)	1237	1103	1090	1070	1062	1045	1048	1053	1054	1054	1023		989	998	954
	TC (°C)	1217	1218	1218	1218	1221	1223	1227	1228	1230	1208	1146		1050	1051	991
	Scale thickness (μm)				9.5	36.2	7.8	29.1	52.0	52.6	73.9	9.1		64.9		66.0
With stop	TM (°C)	1224	1204	1204	1200	1198	1191	1190	1182	1179	1155	1105		1029	1032	920
	TS (°C)	1237	1103	1090	1070	1062	1045	1048	1053	1054	1054	1023		989	998	897
	TC (°C)	1217	1218	1218	1218	1221	1223	1227	1228	1230	1208	1146		1050	1051	931
	Scale thickness (μm)				9.5	36.2	7.8	29.1	52.0	52.6	73.9	9.1		64.9		74.7

4 CONCLUSION

Based on elementary concepts it was possible to develop a simple but accurate model for temperature prediction during rough rolling, the error margin being within 9°C ~ 17°C.

The developed thermal model may be used for estimating the temperature drop of the slab or the transfer bar when it stops temporarily at any location in the roughing line. In case of stopping before the rougher R1, holding for as long as a couple of minutes will cause a small slab temperature drop, not hindering further processing. In case of stopping after the rougher R2, a much shorter stop may render further transfer bar processing unfeasible. As examples, if the slab stops for 148 s the temperature drop of the transfer bar at TS location is approximately 15°C. On the contrary, a short stop of the transfer bar for 48 s after R2 leads to 40º ~ 60°C temperature drop at TS.

So the model can help decision-making about either continuing the rolling schedule or indicating the need to change it.

Further work is needed to implement the model as an online tool to help operators actuate in case of abnormal line stop.

REFERENCES

1 Hollander F. A model to calculate the complete temperature distribution in steel during hot rolling. In: Proceedings of the Mathematical Process Models in Iron and Steelmaking Conference, 1973, Amsterdam, 46-79.

2 Santos AA, Schiavo CP, Giacomin CN. Simulação computacional do processo de reaquecimento de placas em fornos de viga móvel. Tecnologia em Metalurgia e Materiais, 2008, 1: 35-39.

3 Panjkivic V, Gloss R. Fast dynamic heat and mass balance model of walking beam reheat furnace with two-dimensional slab temperature profile. Ironmaking and Steelmaking, 2012, 9:190-209.

4 Ding JG, Zhao Z., Jiao Z., Wang J. Temperature control technology by finite difference scheme with thickness unequally partitioned method in gradient temperature rolling process. ISIJ International, 2017, 7: 1141–1148.

5 Li HJ, Li LG, Li YL, Wang GD. Online monitor and control of cooling temperature on run-out table of hot strip mill. Steel Research Int., 2015, 11: 1225-1233.

6 Li HJ, Li ZL, Yuan G, Wang ZD, Wang GD. Development of new generation cooling control systems after rolling in hot rolled strip based on UFC. Journal of Iron and Steel Research International, 2013, 7: 29-34.

7 Holman J P. Transferência de Calor, tradução L. F. Milanez, McGraw-Hill, do Brasil, 1983.

8 Santos AA, Souza AC, Maia GA. Behavior of tertiary scale in the arc of contact during hot strip rolling. In: Proceedings of 52º Rolling Seminar, ABM WEEK, São Paulo: 02 ~ 04 October, 2017